J. Cent. South Univ. (2015) 22: 1298−1306
DOI: 10.1007/s11771-015-2646-z

Springer

A novel two-degree-of-freedom spherical ultrasonic motor using three travelling-wave type annular stators

WANG Jian(王剑)[1], HU Xi-xing(胡锡幸)[2], WANG Ban(王班)[1], GUO Ji-feng(郭吉丰)[1]

1. College of Electrical Engineering, Zhejiang University, Hangzhou 310027, China;
2. Hangzhou Power Supply Company of State Grid, Zhejiang Electric Power Company, Hangzhou 310009, China

Abstract: In order to promote the tolerance and controllability of the multi-degree-of-freedom (M-DOF) ultrasonic motor, a novel two-degree-of-freedom (2-DOF) spherical ultrasonic motor using three traveling-wave type annular stators was put forward. Firstly, the structure and working principle of this motor were introduced, especially a spiral spring as the preload applied component was designed for adaptive adjustment. Then, the friction drive model of 2-DOF spherical motor was built up from spatial geometric relation between three annular stators and the spherical rotor which was used to analyze the mechanical characteristics of the motor. The optimal control strategy for minimum norm solution of three stators' angular velocity was proposed, using Moore-Penrose generalized inverse matrix. Finally, a 2-DOF prototype was fabricated and tested, which ran stably and controllably. The maximum no-load velocity and stall torque are 92 r/min and 90 mN·m, respectively. The 2-DOF spherical ultrasonic motor has compact structure, easy assembly, good performance and stable operation.

Key words: two-degree-of-freedom; ultrasonic motor; spherical rotor; friction drive model; optimal control strategy

1 Introduction

Using the converse piezoelectric effect of piezoelectric ceramics, ultrasonic motor changes the microscopic transformation of elastic materials into macroscopic motion of the rotor. Ultrasonic motor has many special features, such as low speed, high torque, fast response, high resolution, high power density and no electromagnetic interference [1]. As a result, ultrasonic motors can replace some low-power electromagnetic motors in practice, showing wide application prospects.

The traditional single-DOF motion is difficult to fulfill the rising of industry's requirements for electromechanical equipment. The electromagnetic multi-degree-of-freedom (M-DOF) motors generally desire more complex structure, difficult manufacture and control, high cost, also more complicated gearing [2]. Japanese scholars firstly proposed the use of ultrasonic motor for driving M-DOF motion.

M-DOF ultrasonic motor has merits of high mechanical integration and various realization forms of output motion. In recent years, researchers have proposed a series of structural forms of M-DOF ultrasonic motors, which mostly have a spherical rotor. According to the shape of the stator, the M-DOF spherical ultrasonic motors can be divided into four categories: the cylindrical stator, the plate-shaped stator, the bowl-shaped stator and the annular stator, which are widely used in the fields of micro-robotics [3], medical equipment [4], and detecting device [5]. The cylindrical stator structure was made firstly by AMANO et al [6]. The Langevin transducer is used to sandwich three groups of piezoelectric ceramics. With a combination of two orthogonal bending vibration modes and a longitudinal mode, the spherical rotor generates 3-DOF motion by friction drive of the stator. Subsequent scholars adopted similar ideas for structural improvements and performance optimization [7−9], but the output torques of these motors are generally small. AOYAGI et al [10] invented the motor with a plate-shaped stator. Thick PZT and electrode were coated on aluminum plate (as the stator), and a short cylinder was bonded in the center of the aluminum plate to support and drive the rotor. The motor operates in the three torsional modes of the aluminum plate. TING et al [11] reported a bowl-shaped stator structure of the motor. The cross-shaped piezoelectric ceramics were bonded to external surface of the bowl-shaped stator. Two or three degrees of freedom motion depend on the choice of

Foundation item: Project(51107111) supported by the National Natural Science Foundation of China
Received date: 2014−01−25; **Accepted date:** 2014−05−09
Corresponding author: WANG Jian, Assistant Professor, PhD; Tel: +86−571−87951784; E-mail: wj.james@163.com

vibration modes. In some extent, the efficiency of such motor is relatively low, moreover, the fabrication and control are relatively complex. The concept of annular stator was proposed by TOYAMA et al [12], and it was applied for 2-DOF ultrasonic motors with two or four stators. In the latter motor, two pairs of vertical stators were used to clamp a spherical rotor, and the axis of opposite stators should go through the centre of rotor. Later, a 3-DOF ultrasonic motor with three stators and its drive model were obtained [13−14]. Three stators were made an angle to the *x*-*y* plane and located at 120° intervals around the *z*-axis. Using the travelling-wave type annular stators, HU et al [15] and FU et al [16] from Zhejiang university (China) successfully developed 2-DOF and 3-DOF spherical ultrasonic motors. After some comprehensive comparison, the structure of annular stators is considered as the main direction of M-DOF spherical ultrasonic motor, which is also the research object of this study.

In this work, based upon the ideas from the structure of 3-DOF spherical ultrasonic motor with three stators, the axis of three stators were arranged in the same sphere section, making the motor degenerate into 2-DOF from 3-DOF motion. This novel 2-DOF spherical ultrasonic motor with three stators had good tolerance due to adaptive adjustment ability of the spiral spring. Firstly, the structure and working principle of the motor were introduced. Secondly, the friction drive model was derived and characteristics of the motor were analyzed. Thirdly, an optimal control strategy for minimum norm solution of three stators' angular velocity was proposed to improve the controllability of the motor. Finally, a 2-DOF prototype was fabricated and tested.

2 Structure and working principle

Figure 1 shows the structure of the 2-DOF spherical ultrasonic motor. The motor mainly consists of three stators, a spherical rotor and a preload loading mechanism. The axis of three stators is arranged in the same sphere section, making the motor degenerate into 2-DOF from 3-DOF motion. The rake angle on outer edge of stator can be adjusted to a desired resonance frequency, and stator contacts with spherical rotor on inner edge to improve the efficiency of energy transfer. A *d* 40 mm Si_3N_4 ceramic sphere with lighter mass, better wear resistance and wear non-oxidizability compared to the steel sphere is selected as the spherical rotor. Preload loading mechanism consists of spiral spring, spring sleeve, spring seat and side cover, and the assembly of those components is shown in Fig. 2. The annular stator is fixed to the centre hole of spiral spring, and three pins of the spiral spring are fixed to the spring sleeve that could move axially in the spring seat. Spring seat is

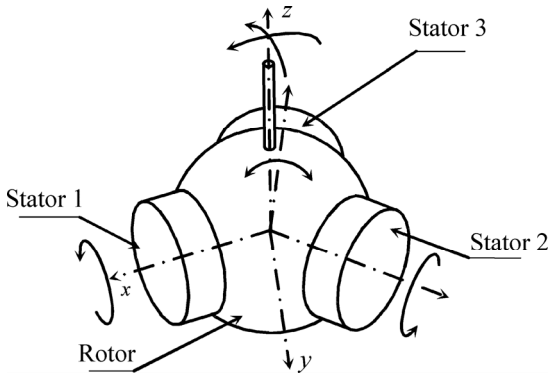

Fig. 1 Sketch of structure and working principle of 2-DOF spherical ultrasonic motor

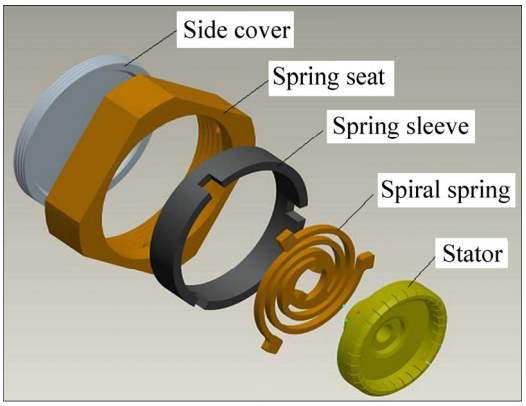

Fig. 2 Preload loading mechanism and its components assembly

mounted on the base. By screwing the side cover, the displacement of the spring sleeve could be adjusted, and then the spiral spring is compressed, so the preload between the stator and rotor is controllable.

Due to the fact that the amplitude of vibration is only few microns when travelling wave type stator is working, inner edge of stator should be kept in touch with spherical rotor closely. Limited by the precision of fabrication and assembly, it is difficult to fully guarantee that the axis of three stators could stay in the same plane and go through the globe of rotor simultaneously. The adaptive adjustment mechanism of spiral spring is introduced to provide the uniform preload, which not only ensures the axial preload, but also overcomes the shortage of micro deflection of the stator's axis. The material of the spiral spring is 65Mn steel, the toughness and fatigue resistance of which are enhanced after hardening and drawing temper. Each spiral spring has three Archimedean screws to be stressed uniformly at the center hole so that it may obtain similar torsional stiffness. So, the spiral spring could ensure the annular stator and spherical rotor center automatically to increase the tolerance during the assembly process of the 2-DOF spherical ultrasonic motor. The spiral spring that directly

affects the output performance of the spherical motor is one of the key components in such design.

When one stator is excited by two sinusoidal signals, the temporal and spatial phase shift of which are both 90° and the remaining two stators are excited by standing wave signals, the particle on surface of inner edge of the first stator could frictionally drive the spherical rotor to rotate around the stator's central axis. By changing the amplitude and phase shift of excitation voltage, the velocity and direction of the rotor's motion can be controlled. This is the basic working principle of the 2-DOF spherical motor with three stators. If three stators are excited simultaneously according to a certain optimal control strategy, the spherical rotor can rotate in any direction of the *x*-*y* plane smoothly and efficiently.

3 Friction drive model

The spatial geometric relation between the stator and rotor of 2-DOF spherical ultrasonic motor is shown in Fig. 3. The origin O of basic coordinate system $\Sigma_0(Oxyz)$ locates at the centre of spherical rotor; R stands for the radius of spherical rotor; S stands for the contact circumference between the stator and rotor with its center O_1; r stands for the effective radius of stator (also the contact circumference S); the axis of Stator 1 is in the plane Oxz; A is the crossing point of contact circumference S and plane Oxz; φ is the included angle of line OA and O_1A; P is an arbitrary point at the contact circumference S; θ is the included angle of line O_1P and O_1A.

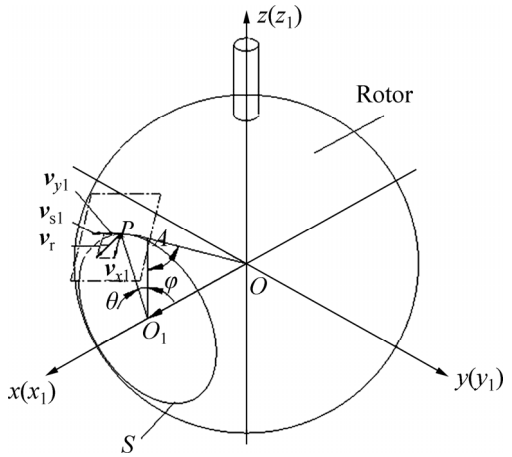

Fig. 3 Spatial geometric relation of 2-DOF spherical motor

The local coordinate system $\Sigma_1(Ox_1y_1z_1)$ of Stator 1 is established as follows: z_1-axis is consistant with the z-axis, then the basic coordinate system $\Sigma_0(Oxyz)$ rotates around z-axis, and finally x_1-axis (the central axis of the stator1) coincides with the x-axis.

Three stators are symmetrical in the spatial position, so it is typical to analyze drive model of the Stator 1. In the local coordinate system $\Sigma_1(Ox_1y_1z_1)$, the position of P can be expressed as

$$\boldsymbol{P}_{\theta 1} = R[\sin\varphi \quad -\cos\varphi\sin\theta \quad \cos\varphi\cos\theta]^{\mathrm{T}} \tag{1}$$

Assume that stator and rotor only rigidly contact at the crest of travelling wave, the angular velocity of contact point on Stator 1 is $\boldsymbol{\omega}_{\mathrm{s1}}$. In the local coordinate system $\Sigma_1(Ox_1y_1z_1)$, the velocity of Stator 1 can be expressed as

$$\boldsymbol{v}_{\mathrm{s1}} = \boldsymbol{\omega}_{\mathrm{s1}} \times \boldsymbol{P}_{\theta 1} \tag{2}$$

Let $\boldsymbol{\omega}_{\mathrm{r}} = [\omega_1 \quad \omega_2 \quad 0]^{\mathrm{T}}$ denote the angular velocity of the spherical rotor in the basic coordinate system $\Sigma_0(Oxyz)$. Since $\Sigma_0(Oxyz)$ coincides with $\Sigma_1(Ox_1y_1z_1)$, the velocity of the spherical rotor in the local coordinate system $\Sigma_1(Ox_1y_1z_1)$ can be expressed as

$$\boldsymbol{v}_{\mathrm{r}} = \boldsymbol{\omega}_{\mathrm{r}} \times \boldsymbol{P}_{\theta 1} \tag{3}$$

In Ref. [17], the torque was transferred with a relative slip between the stator and the rotor, and the theory of friction drive was applied for the model. The friction force $\boldsymbol{F}$ between the stator and rotor can be generally expressed as

$$\boldsymbol{F} = \varepsilon(\boldsymbol{v}_{\mathrm{s}} - \boldsymbol{v}_{\mathrm{r}})F_{\mathrm{n}} \tag{4}$$

where ε is the friction coefficient, F_{n} is the normal positive pressure of contact point, $\boldsymbol{v}_{\mathrm{s}}$ is the velocity of the stator, and $\boldsymbol{v}_{\mathrm{r}}$ is the velocity of the rotor.

$\boldsymbol{v}_{\mathrm{r}}$ can be decomposed into two parts: $\boldsymbol{v}_{y1}$ is with the same direction of the Stator 1 velocity $\boldsymbol{v}_{\mathrm{s1}}$, and $\boldsymbol{v}_{x1}$ is perpendicular to the direction of the stator velocity. The Stator 1 generates a driving force $\boldsymbol{F}_{\mathrm{d1}}$ to the rotor:

$$\boldsymbol{F}_{\mathrm{d1}} = \varepsilon(\boldsymbol{v}_{\mathrm{s1}} - \boldsymbol{v}_{y1})F_{\mathrm{n1}} \tag{5}$$

where F_{n1} is the normal positive pressure of contact point between Stator 1 and rotor.

Therefore, the driving torque generated by Stator 1 can be expressed as

$$\boldsymbol{T}_{\mathrm{d1}} = \frac{n}{2\pi}\int_0^{2\pi} \boldsymbol{P}_{\theta 1} \times \boldsymbol{F}_{\mathrm{d1}}\mathrm{d}\theta = \frac{n\varepsilon F_{\mathrm{n1}}R^2}{2}\begin{bmatrix} 2(\omega_{\mathrm{s1}} - \omega_1)\cos^2\varphi \\ -\omega_2\sin^2\varphi \\ 0 \end{bmatrix} \tag{6}$$

where n represents the order of the stator's vibration mode.

The spherical rotor and Stator 1 have the velocity difference at the contact point P, along the $\boldsymbol{v}_{x1}$ direction. So Stator 1 generates resistance force $\boldsymbol{F}_{\mathrm{f1}}$ to the spherical rotor:

$$\boldsymbol{F}_{\mathrm{f1}} = \varepsilon(0 - \boldsymbol{v}_{x1})F_{\mathrm{n1}} \tag{7}$$

Accordingly, the resistance torque $\boldsymbol{T}_{\mathrm{f1}}$ can be

expressed as

$$\boldsymbol{T}_{\mathrm{f1}}=\frac{n}{2\pi}\int_0^{2\pi}\boldsymbol{P}_{\theta 1}\times\boldsymbol{F}_{\mathrm{f1}}\mathrm{d}\theta=-\frac{n\varepsilon F_{\mathrm{n1}}R^2\omega_2}{2}\begin{bmatrix}0\\1\\0\end{bmatrix} \tag{8}$$

Stator 1 generates total torque $\boldsymbol{T}_1$ to the spherical rotor, which can be expressed as

$$\boldsymbol{T}_1=\boldsymbol{T}_{\mathrm{d1}}+\boldsymbol{T}_{\mathrm{f1}}=\frac{n\varepsilon F_{\mathrm{n1}}R^2}{2}\begin{bmatrix}2(\omega_{\mathrm{s1}}-\omega_1)\cos^2\varphi\\-\omega_2\sin^2\varphi-\omega_2\\0\end{bmatrix} \tag{9}$$

From Eqs. (6), (8) and (9), it can be seen that the torque $\boldsymbol{T}_1$ has the component in the x_1-axis and y_1-axis directions, while there is none in the z_1-axis direction. Thus, the following derivation is represented by two-dimension, which is in accordance with the concept of 2-DOF motor. So, $\boldsymbol{T}_1$ can be redefined as follows:

$$\boldsymbol{T}_1=\frac{n\varepsilon F_{\mathrm{n1}}R^2}{2}\begin{bmatrix}2(\omega_{\mathrm{s1}}-\omega_1)\cos^2\varphi\\-\omega_2\sin^2\varphi-\omega_2\end{bmatrix} \tag{10}$$

The transformation matrix $\boldsymbol{A}_{01}$ transforms the basic coordinate system $\Sigma_0(Oxyz)$ into the local coordinate system $\Sigma_1(Ox_1y_1z_1)$:

$$\boldsymbol{A}_{01}=\begin{bmatrix}1&0\\0&1\end{bmatrix} \tag{11}$$

In the local coordinate system $\Sigma_1(Ox_1y_1z_1)$, Stator 1 generates the total torque T_{01} to the spherical rotor, which can be expressed as

$$\boldsymbol{T}_{01}=\boldsymbol{A}_{01}\cdot\boldsymbol{T}_1=\frac{n}{2}\varepsilon F_{\mathrm{n1}}R^2\begin{bmatrix}2\omega_{\mathrm{s1}}\cos^2\varphi-2\omega_1\cos^2\varphi\\-\omega_2\sin^2\varphi-\omega_2\\0\end{bmatrix} \tag{12}$$

The local coordinate system $\Sigma_2(Ox_2y_2z_2)$ of Stator 2 is established as follows: the basic coordinate system $\Sigma_0(Oxyz)$ rotates 120° counter-clockwise (CCW) around z-axis, and x_2-axis (the central axis of the Stator 2) coincides with the x-axis. The transformation matrix A_{02} can be expressed as

$$\boldsymbol{A}_{02}=\begin{bmatrix}-1/2&-\sqrt{3}/2\\\sqrt{3}/2&-1/2\end{bmatrix} \tag{13}$$

The basic coordinate system $\Sigma_0(Oxyz)$ rotates 240° CCW around z-axis, and the local coordinate system $\Sigma_3(Ox_3y_3z_3)$ of Stator 3 is obtained. The transformation matrix $\boldsymbol{A}_{03}$ can be expressed as

$$\boldsymbol{A}_{03}=\begin{bmatrix}-1/2&\sqrt{3}/2\\-\sqrt{3}/2&-1/2\end{bmatrix} \tag{14}$$

The analysis method of Stator 2 and Stator 3 is consistent with that of Stator 1, and the results would be given directly. The driving torque $\boldsymbol{T}_{\mathrm{d2}}$, the resistance torque $\boldsymbol{T}_{\mathrm{f2}}$, and the total torque $\boldsymbol{T}_{02}$ of the Stator 2 are respectively expressed as

$$\boldsymbol{T}_{\mathrm{d2}}=\frac{n\varepsilon F_{\mathrm{n2}}R^2}{2}\begin{bmatrix}-\omega_{\mathrm{s2}}\cos^2\varphi-\frac{1}{2}\omega_1+\frac{\sqrt{3}}{2}\omega_2-\\\frac{1}{4}\sin^2\varphi\omega_1-\frac{3\sqrt{3}}{4}\sin^2\varphi\omega_2\\\sqrt{3}\omega_{\mathrm{s2}}\cos^2\varphi+\frac{\sqrt{3}}{2}\omega_1-\frac{3}{2}\omega_2-\\\frac{3\sqrt{3}}{4}\sin^2\varphi\omega_1+\frac{5}{4}\sin^2\varphi\omega_2\end{bmatrix} \tag{15}$$

$$\boldsymbol{T}_{\mathrm{f2}}=-\frac{n\varepsilon F_{\mathrm{n2}}R^2}{2}\begin{bmatrix}\frac{3}{4}\omega_1+\frac{\sqrt{3}}{4}\omega_2\\\frac{\sqrt{3}}{4}\omega_1+\frac{1}{4}\omega_2\end{bmatrix} \tag{16}$$

$$\boldsymbol{T}_{02}=\boldsymbol{T}_{\mathrm{d2}}+\boldsymbol{T}_{\mathrm{f2}}=\frac{n\varepsilon F_{\mathrm{n2}}R^2}{2}\begin{bmatrix}-\omega_{\mathrm{s2}}\cos^2\varphi-\frac{1}{4}\sin^2\varphi\omega_1-\\\frac{3\sqrt{3}}{4}\sin^2\varphi\omega_2-\frac{5}{4}\omega_1+\frac{\sqrt{3}}{4}\omega_2\\\sqrt{3}\omega_{\mathrm{s2}}\cos^2\varphi-\frac{3\sqrt{3}}{4}\sin^2\varphi\omega_1+\\\frac{5}{4}\sin^2\varphi\omega_2+\frac{\sqrt{3}}{4}\omega_1-\frac{7}{4}\omega_2\end{bmatrix} \tag{17}$$

Also, the driving torque $\boldsymbol{T}_{\mathrm{d3}}$, the resistance torque $\boldsymbol{T}_{\mathrm{f3}}$, and the total torque $\boldsymbol{T}_{03}$ of the Stator 3 are respectively expressed as

$$\boldsymbol{T}_{\mathrm{d3}}=\frac{n\varepsilon F_{\mathrm{n3}}R^2}{2}\begin{bmatrix}-\omega_{\mathrm{s3}}\cos^2\varphi-\frac{1}{2}\omega_1-\frac{\sqrt{3}}{2}\omega_2-\\\frac{1}{4}\sin^2\varphi\omega_1+\frac{3\sqrt{3}}{4}\sin^2\varphi\omega_2\\-\sqrt{3}\omega_{\mathrm{s3}}\cos^2\varphi-\frac{\sqrt{3}}{2}\omega_1-\frac{3}{2}\omega_2+\\\frac{3\sqrt{3}}{4}\sin^2\varphi\omega_1+\frac{5}{4}\sin^2\varphi\omega_2\end{bmatrix} \tag{18}$$

$$\boldsymbol{T}_{\mathrm{f3}}=-\frac{n\varepsilon F_{\mathrm{n3}}R^2}{2}\begin{bmatrix}\frac{3}{4}\omega_1-\frac{\sqrt{3}}{4}\omega_2\\-\frac{\sqrt{3}}{4}\omega_1+\frac{1}{4}\omega_2\end{bmatrix} \tag{19}$$

$$\boldsymbol{T}_{03}=\boldsymbol{T}_{\mathrm{d3}}+\boldsymbol{T}_{\mathrm{f3}}=\frac{n\varepsilon F_{\mathrm{n3}}R^2}{2}\begin{bmatrix}-\omega_{\mathrm{s3}}\cos^2\varphi-\frac{1}{4}\sin^2\varphi\omega_1+\\\frac{3\sqrt{3}}{4}\sin^2\varphi\omega_2-\frac{5}{4}\omega_1-\frac{\sqrt{3}}{4}\omega_2\\-\sqrt{3}\omega_{\mathrm{s3}}\cos^2\varphi+\frac{3\sqrt{3}}{4}\sin^2\varphi\omega_1+\\\frac{5}{4}\sin^2\varphi\omega_2-\frac{\sqrt{3}}{4}\omega_1-\frac{7}{4}\omega_2\end{bmatrix} \tag{20}$$

The output torque $\boldsymbol{T}$ of 2-DOF spherical ultrasonic motor can be expressed as

$$\boldsymbol{T}=\boldsymbol{T}_{01}+\boldsymbol{T}_{02}+\boldsymbol{T}_{03} \tag{21}$$

Each stator of the motor is force balanced in the axial direction as

$$\frac{n}{2\pi}\int_0^{2\pi}(F_{\mathrm{n}i}\boldsymbol{P}_{\theta i}-\boldsymbol{F}_{\mathrm{d}i}-\boldsymbol{F}_{\mathrm{f}i})\cdot\boldsymbol{x}_i\mathrm{d}\theta=F_{\mathrm{c}i}\quad(i=1,\ 2,\ 3) \tag{22}$$

where $\boldsymbol{x}_i$ is the unit vector from centre of sphere O to the centre of stator i, $F_{\mathrm{c}i}$ is the preload applied for the stator i. Generally speaking, $F_{\mathrm{c}1}=F_{\mathrm{c}2}=F_{\mathrm{c}3}$, so the spherical rotor is force balanced (excluding the gravity of the rotor). The normal positive pressure $F_{\mathrm{n}i}$ can be solved by Eq. (22), and it is easy to get $F_{\mathrm{n}1}=F_{\mathrm{n}2}=F_{\mathrm{n}3}$.

Combining Eqs. (12), (17), (20), (21) and (22), the output torque of motor $\boldsymbol{T}$ can be expressed as

$$\boldsymbol{T}=\frac{n\varepsilon F_{\mathrm{n}1}R^2}{2}\begin{bmatrix}\cos^2\varphi(2\omega_{\mathrm{s}1}-\omega_{\mathrm{s}2}-\omega_{\mathrm{s}3})+(\frac{3}{2}\sin^2\varphi-\frac{9}{2})\omega_1\\ \sqrt{3}\cos^2\varphi(\omega_{\mathrm{s}2}-\omega_{\mathrm{s}3})+(\frac{3}{2}\sin^2\varphi-\frac{9}{2})\omega_2\end{bmatrix} \tag{23}$$

4 Analysis of characteristics

In order to verify the validity and effectiveness of the friction drive model, a set of structure parameters are taken into account to analyze the characteristics of the motor, as listed in Table 1.

Table 1 Model parameters for simulation

Parameter	Value
R/mm	20
r/mm	11
ε	0.15
n	5
F_{c}/N	30

4.1 No-load velocity of motor

When the motor is running without any load (T=0), the no-load velocity $\boldsymbol{\omega}_{\mathrm{r}0}$ of the spherical motor can be obtained by

$$\boldsymbol{\omega}_{\mathrm{r}0}=\begin{pmatrix}\omega_{10}\\ \omega_{20}\end{pmatrix}=\begin{pmatrix}2k & -k & -k\\ 0 & \sqrt{3}k & -\sqrt{3}k\end{pmatrix}\begin{pmatrix}\omega_{\mathrm{s}1}\\ \omega_{\mathrm{s}2}\\ \omega_{\mathrm{s}3}\end{pmatrix} \tag{24}$$

where $k=\cos^2\varphi/(9/2-3\sin^2\varphi/2)$.

The value of the no-load velocity of the spherical motor depends on the angular velocity of three stators. The no-load velocity could be controlled by adjusting the angular velocity of three stators.

4.2 Stall torque of motor

When the motor is stalled, the angular velocity of the spherical rotor is zero ($\omega_{\mathrm{r}}=0$). The stall torque $\boldsymbol{T}_0$ of the spherical motor also can be obtained by

$$\boldsymbol{T}_0=\begin{pmatrix}T_{10}\\ T_{20}\end{pmatrix}=\begin{pmatrix}2k' & -k' & -k'\\ 0 & \sqrt{3}k' & -\sqrt{3}k'\end{pmatrix}\begin{pmatrix}\omega_{\mathrm{s}1}\\ \omega_{\mathrm{s}2}\\ \omega_{\mathrm{s}3}\end{pmatrix} \tag{24}$$

where $k'=n\varepsilon F_{\mathrm{n}1}R^2\cos^2\varphi/2$.

Once the values of the motor structure parameters and the preload are determined, the stall torque of the spherical motor also depends on the angular velocity of three stators.

4.3 Direction of angular velocity $\boldsymbol{\omega}_{\mathrm{r}0}$

Assume that $|\omega_{\mathrm{s}1}|\le 1$, $|\omega_{\mathrm{s}2}|\le 1$, $|\omega_{\mathrm{s}3}|\le 1$, and ψ is the angle of no-load velocity $\boldsymbol{\omega}_{\mathrm{r}0}$ and x-axis ($\tan\psi=\omega_{20}/\omega_{10}$). The relation between the maximum of no-load velocity $\boldsymbol{\omega}_{\mathrm{r}0}$ and the angle ψ is shown in Fig. 4.

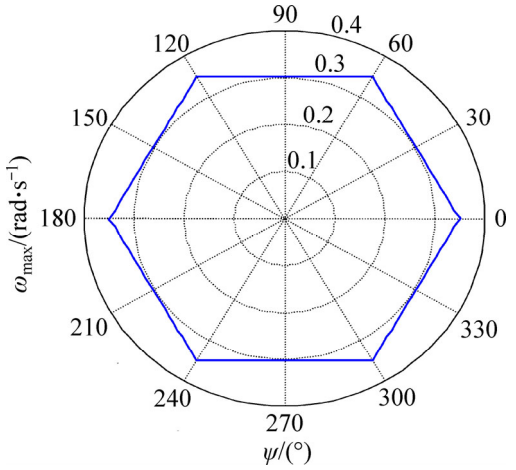

Fig. 4 Relation between maximum of $\boldsymbol{\omega}_{\mathrm{r}0}$ and angle ψ

The maxima of no-load velocity uniformly distribute at the angles of 0°, 60°, 120°, 180°, 240° and 300°. When the motor is running at the max velocity shown in Fig. 4, the angular velocities of three stators $\boldsymbol{\omega}_{\mathrm{s}i}$ are shown in Fig. 5. The right figures are enlarged parts of angle $\psi\in[0°, 30°]$.

5 Redundancy and control strategy

This spherical ultrasonic motor realizes the 2-DOF motion using three annular stators, so that one of stators is redundant. According to different optimal goals, there are corresponding solutions to satisfy Eq. (24). Aiming at the maximum of no-load velocity $\boldsymbol{\omega}_{\mathrm{r}0}$ in the previous section, the result is one group of solutions. However,

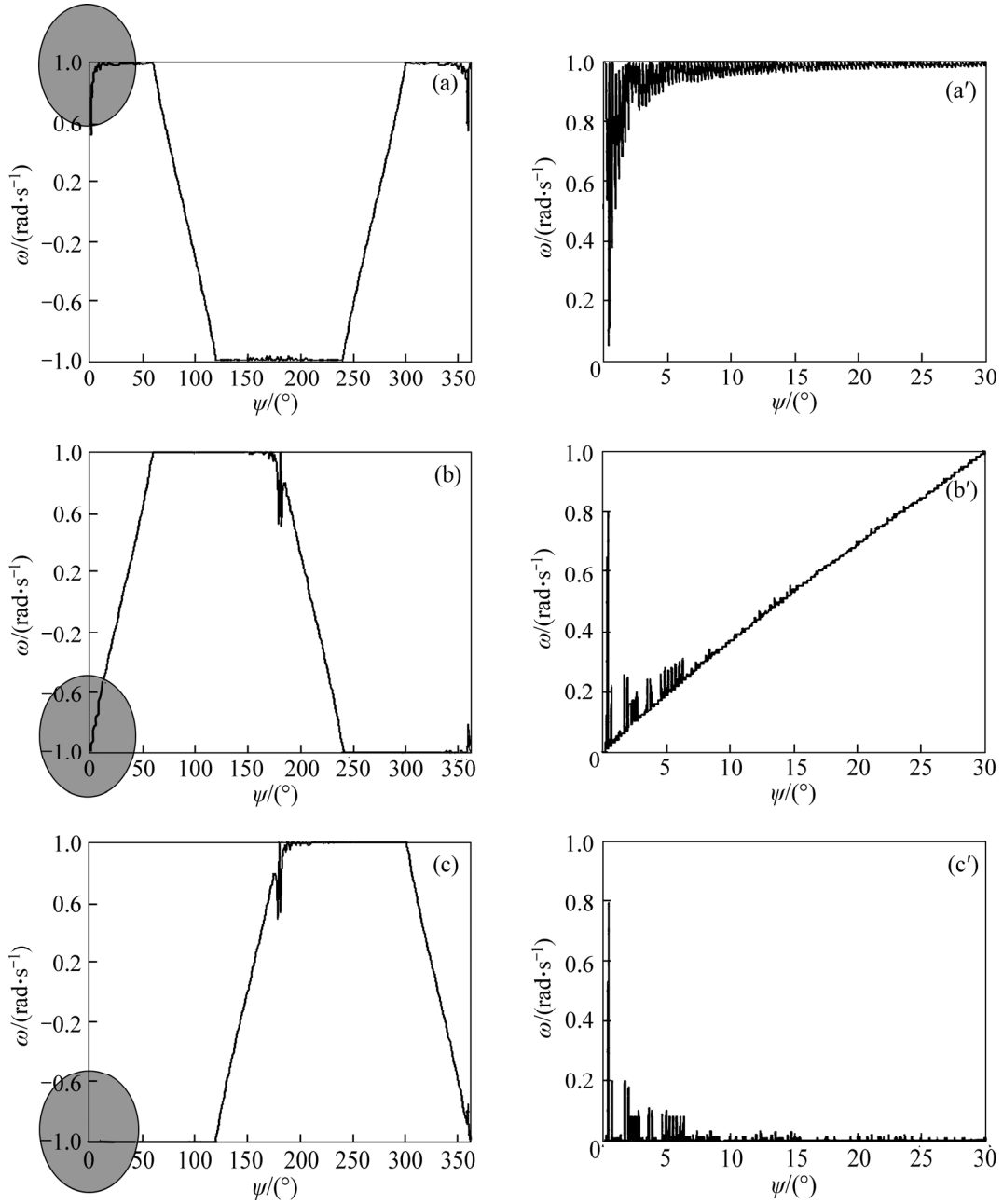

Fig. 5 Relation between angular velocity ω and angle ψ: (a, a′) ω_{s1}; (b, b′) ω_{s2}; (c, c′) ω_{s3}

under the above optimal framework, it is somehow difficult to control the result, because the values of three stators' angular velocity mutate in different directions, especially in 0° and 180°.

An optimal control strategy for minimum norm solution of three stators' angular velocity is proposed, using Moore-Penrose generalized inverse matrix. $\boldsymbol{A}$ is a full row rank matrix, thus its Moore-Penrose generalized inverse matrix $\boldsymbol{A}^+$ can be expressed as

$$\boldsymbol{A}^+ = \boldsymbol{A}^{\mathrm{T}}(\boldsymbol{A}\cdot\boldsymbol{A}^{\mathrm{T}})^{-1} = \frac{1}{6k}\begin{pmatrix} 2 & 0 \\ -1 & \sqrt{3} \\ -1 & -\sqrt{3} \end{pmatrix} \tag{26}$$

where $\boldsymbol{A} = \begin{pmatrix} 2k & -k & -k \\ 0 & \sqrt{3}k & -\sqrt{3}k \end{pmatrix}$.

When the no-load velocity of the spherical rotor is limited within the unit circle, $\boldsymbol{\omega}_{r0}=[\omega_{10}\ \omega_{20}]^{\mathrm{T}}=1\angle\psi$. The expression of the ω_{s1}, ω_{s2}, ω_{s3} could be given, according to Eq. (27). The relations of angular velocity ω_{si} and angle ψ are shown in Fig. 6.

$$\begin{pmatrix} \omega_{s1} \\ \omega_{s2} \\ \omega_{s3} \end{pmatrix} = \boldsymbol{A}^+\begin{pmatrix} \omega_{10} \\ \omega_{20} \end{pmatrix} = \frac{1}{6k}\begin{pmatrix} 2 & 0 \\ -1 & \sqrt{3} \\ -1 & -\sqrt{3} \end{pmatrix}\begin{pmatrix} \cos\psi \\ \sin\psi \end{pmatrix}$$

$$=\frac{1}{3k}\begin{pmatrix}\cos\psi\\ \cos(\psi-120^\circ)\\ \cos(\psi-240^\circ)\end{pmatrix} \quad (27)$$

Substituting Eq. (27) into Eq. (23), the total torque of the motor is obtained.

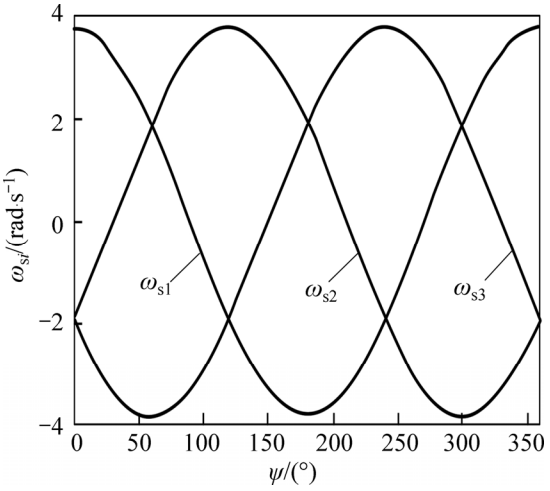

Fig. 6 Relation between angular velocity ω_{si} and angle ψ

$$\boldsymbol{T}=\frac{n}{2}\varepsilon F_{n1}R^2\begin{pmatrix}\frac{1}{k}\cos^2\varphi\cos\psi+(\frac{3}{2}\sin^2\varphi-\frac{9}{2})\omega_1\\ \frac{1}{k}\cos^2\varphi\sin\psi+(\frac{3}{2}\sin^2\varphi-\frac{9}{2})\omega_2\end{pmatrix} \quad (28)$$

By this control strategy, the value of the motor's stall torque is constant and independent of the direction of the no-load velocity.

$$\boldsymbol{T}_0=\frac{n}{2k}\cos^2\varphi\cdot\varepsilon F_{n1}R^2\angle\psi=3.73\angle\psi \quad (29)$$

The trajectories of $\boldsymbol{T}_{d1}$, $\boldsymbol{T}_{d2}$, $\boldsymbol{T}_{d3}$, $\boldsymbol{T}_{f1}$, $\boldsymbol{T}_{f2}$ and $\boldsymbol{T}_{f3}$ changing with angle ψ are shown in Figs. 7 and 8, respectively. The direction of the arrow indicates the direction of the trajectory movement.

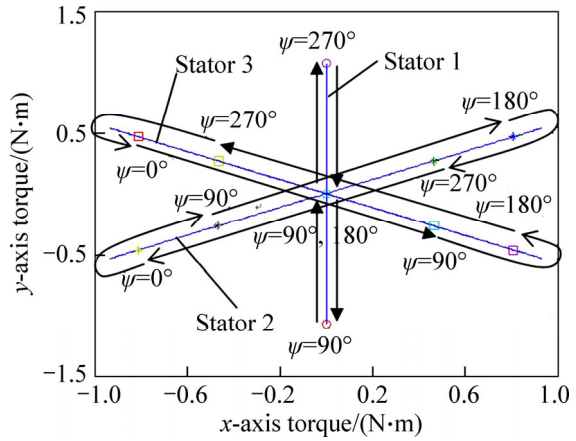

Fig. 7 Trajectories of resistance torque of three stators

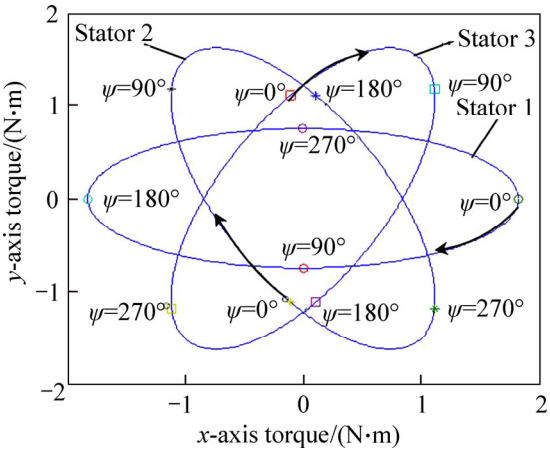

Fig. 8 Trajectories of driving torque of three stators

6 Prototype testing

The motor prototype is fabricated, as shown in Fig. 9, the dimensions of which are 5.2 cm × 8.5 cm × 8.1 cm, wherein stator diameter is 30 mm (effective diameter of the contact circumference is 22 mm), rotor diameter is 40 mm, and mass is 544 g. The performance of the spherical motor is demonstrated by a specialized experimental setup which measures the mechanical characteristics. The method for testing the torque is based on pressure sensors, and rotary encoders are used to measure the rotary velocity and position. The motor driving circuit applies an AC sinusoidal voltage (V_{pp}= 350 V) at resonance frequency (f=49 kHz) to three stators. The circuit equips a phase difference shifter which can change the rotational direction and magnitude of the spherical rotor's rotary velocity. The mechanical characteristics of the motor are tested when the spherical rotor rotates around x-axis and y-axis respectively, according to the control strategy. Figure 10 shows the mechanical characteristics of the motor under different preloads F_c. As the preload increases, the no-load velocity reduces but the stall torque increases significantly. The maximum no-load velocity of the

Fig. 9 Prototype of 2-DOF spherical ultrasonic motor

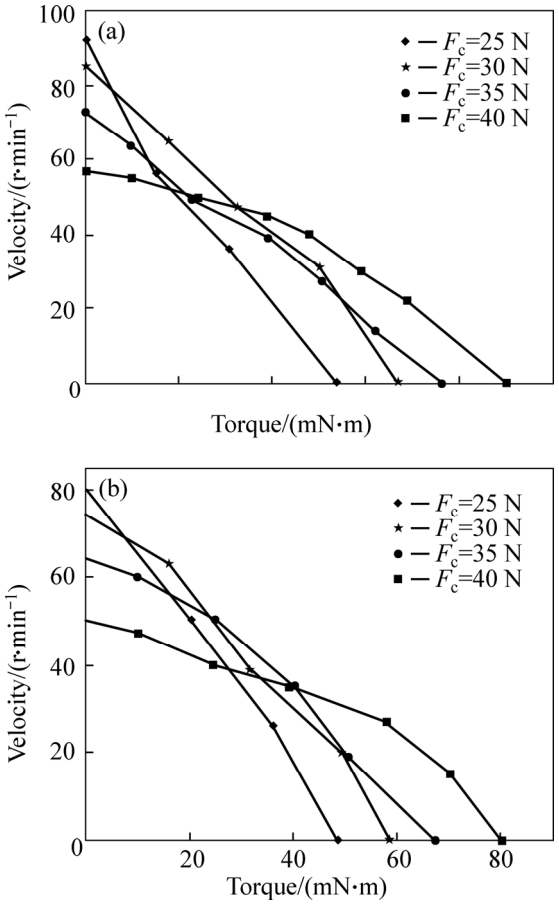

Fig. 10 Mechanical characteristics of motor under different preloads: (a) *x*-axis; (b) *y*-axis

motor is 92 r/min and stall torque is 90 mN·m. The spherical motor has compact structure, easy assembly, good performance and stable operation.

7 Conclusions

1) A novel 2-DOF spherical ultrasonic motor using three travelling wave type annular stators is present to improve the tolerance and controllability of M-DOF motor. According to the spatial relation and coordinate transformation, the motor friction drive mathematical model is established and simulation of the motor characteristics is analyzed.

2) The proposed structure of the spiral spring has the adaptive capacity, which guarantees that the inner edge of the stator closely fits the spherical rotor to provide the uniform preload between the stator and rotor. The spiral spring could ensure that the annular stator and spherical rotor center could automatically increase the tolerance during the assembly process of the 2-DOF spherical ultrasonic motor.

3) The optimal control strategy for minimum norm solution of three stators' angular velocity is proposed based on the friction drive model. This control strategy makes motor have better controllability.

4) This motor omits a stator compared to the traditional 2-DOF motor which has four stators, so the structure is more simple and compact with high reliability. Its no-load velocity and stall torque are basically the same with traditional four-stator motors, so this motor has good performance and controllability. In addition, this motor runs smoothly with reasonable stability. Therefore, the motor has broad application prospects in the fields of micro-robot and CCD control.

References

[1] SHI Yun-lai, CHEN Chao, ZHAO Chun-sheng. Optimal design of butterfly-shaped linear ultrasonic motor using finite element method and response surface methodology [J]. Journal of Central South University, 2013, 20(2): 393−404.

[2] GUO Ji-feng, BAI Yang, WANG Jian. Recent development and prospect of multi-degree-of-freedom ultrasonic motors [J]. Journal of Vibration and Shock, 2013, 32(15): 1−7. (in Chinese)

[3] ZHANG Xiao-feng, NAKAMURA K, UEHA S. Two-joint robot finger design based on multi-degree-of-freedom ultrasonic motors [J]. Acoustical Science and Technology, 2009, 30(1): 42−47.

[4] TAKEMURA K, PARK S, MAENO T. Control of multi-DOF ultrasonic actuator for dexterous surgical instrument [J]. Journal of Sound and Vibration, 2008, 311(3/4/5): 652−666.

[5] HOSHINA M, MASHIMO T, FUKAYA N, MATSUBARAD O, TOYAMA S. Spherical ultrasonic motor drive system for camera orientation in pipe inspection [J]. Advanced Robotics, 2013, 27(3): 199−209.

[6] AMANO T, ISHII T, NAKAMURA K, UEHA S. An ultrasonic actuator with multi degree of freedom using bending and longitudinal vibrations of a single stator [C]// Proceedings of the Ultrasonics Symposium. Sendai: IEEE, 1998: 667−670.

[7] XU Zhi-ke, JIN Long, HU Min-qiang, GU Ju-ping. Research on a novel 3-DOF ultrasonic motor with two cylinder stators [J]. Micromotors, 2009, 42(4): 27−29. (in Chinese)

[8] LI Zhi-rong, ZHAO Chun-sheng, HUANG Wei-qing. Structural dynamics optimal design of a 3-DOF cylinder type stator of ultrasonic motor [J]. Journal of Vibration and Engineering, 2005, 18(4): 471−474. (in Chinese)

[9] GOUDA Y, NAKAMURA K, UEHA S. A miniaturization of the multi-degree-of-freedom ultrasonic actuator using a small cylinder fixed on a substrate [J]. Ultrasonics, 2006, 44(Supplement): e617−e620.

[10] AOYAGI M, BEEBY S P, WHITE N M. A novel multi-degree-of-freedom thick-film ultrasonic motor [J]. IEEE Transactions on Ultrasonics, Ferroelectrics and Frequency Control, 2002, 49(2): 151−158.

[11] TING Y, TSAI Y R, HOU B K, LIN S C, LU C C. Stator design of a new type of spherical piezoelectric motor [J]. IEEE Transactions on Ultrasonics, Ferroelectrics and Frequency Control, 2010, 57(10): 2334−2342.

[12] TOYAMA S, SHIGERU S, ZHANG Guo-qing, MIYATANI Y, NAKAMURA K. Multi degree of freedom spherical ultrasonic motor [C]// Proceedings of IEEE International Conference on Robotics and

Automation. Nagoya: IEEE, 1995: 2935−2940..

[13] PURWANTO E, TOYAMA S. Control method of a spherical ultrasonic motor [C]// Proceedings of 2003 IEEE/ASME International Conference on Advanced Intelligent Mechatronics. Kobe: IEEE, 2003: 1321−1326.

[14] MASHIMO T, TOYAMA S, ISHIDA H. Design and implementation of spherical ultrasonic motor [J]. IEEE Transactions on Ultrasonics, Ferroelectrics and Frequency Control, 2009, 56(11): 2514−2521.

[15] HU Xi-xing, GUO Ji-feng, FU Ping, SHEN Run-jie. Mechanical characteristics calculation of 2-DOF spherical traveling-wave type ultrasonic motor [J]. Journal of Mechanical Engineering, 2010, 45(3): 229−233. (in Chinese)

[16] FU Ping, GUO Ji-feng, SHEN Run-jie. Statics analysis of three-degree-of-freedom traveling-wave type ultrasonic motor [J]. Journal of Zhejiang University (Engineering Science), 2007, 41(6): 968−972. (in Chinese)

[17] MINORU K, SADAYUKI U. Efficiency of ultrasonic motor using traveling wave [J]. Journal of the Acoustical Society of Japan, 1988, 44(1): 40−46.

(Edited by FANG Jing-hua)